Article
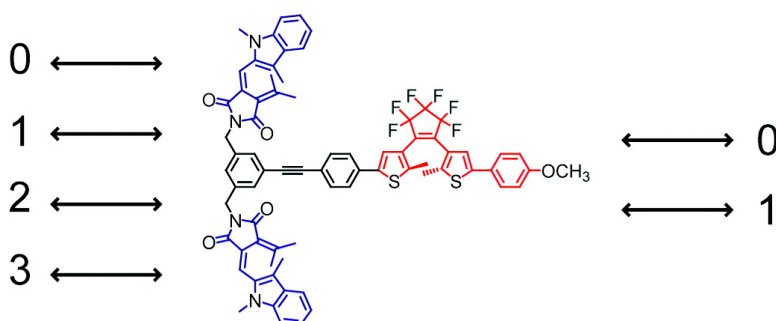
Molecular All-Photonic Encoder#Decoder

Joakim Andre#asson, Stephen D. Straight, Thomas A. Moore, Ana L. Moore, and Devens Gust

More About This Article

Additional resources and features associated with this article are available within the HTML version:

- Supporting Information
- Links to the 1 articles that cite this article, as of the time of this article download
- Access to high resolution figures
- Links to articles and content related to this article
- Copyright permission to reproduce figures and/or text from this article

View the Full Text HTML

Molecular All-Photonic Encoder–Decoder

Joakim Andréasson,*,† Stephen D. Straight,‡ Thomas A. Moore,*,‡ Ana L. Moore,*,‡
and Devens Gust*,‡

*Department of Chemical and Biological Engineering, Chalmers University of Technology,
SE-412 96 Göteborg, Sweden, and Department of Chemistry and Biochemistry,
Arizona State University, Tempe, Arizona 85287-1604*

Received April 17, 2008; E-mail: a-son@chalmers.se; gust@asu.edu; tom.moore@asu.edu; amoore@asu.edu

Abstract: In data processing, an encoder can compress digital information for transmission or storage, whereas a decoder recovers the information in its original form. We report a molecular triad consisting of a dithienylethene covalently linked to two fulgimide photochromes that performs as an all-photonic single-bit 4-to-2 encoder and 2-to-4 decoder. The encoder compresses the information contained in the four inputs into two outputs. The inputs are light of four different wavelengths that photoisomerize the fulgimide, dithienylethene, or both. The outputs are absorbance at two wavelengths. The two decoder inputs are excitation at two wavelengths, whereas the four outputs, which recover the information compressed into the inputs, are absorbance at two wavelengths, transmittance at one wavelength, and fluorescence emission. The molecule can be cycled through numerous encoder and decoder functions without significant photodecomposition. Molecular photonic encoders and decoders could potentially be used for labeling and tracking of nano- and microscale objects as well as for data manipulation.

Introduction

It is becoming well-established that because some molecules can act as reversible switches in response to stimuli, they can be used to perform digital data-processing functions, much as is done by the transistor switches in conventional electronics. Molecular switches, Boolean logic gates, and other data manipulation devices have been described.[1–11] Although most of the initial reports of such systems were of simple switches or single-function logic gates, more recent work has produced molecules or mixtures of molecules capable of performing a variety of logic functions.[12–19] Most often, these systems use

Table 1. Truth Table for the 4-to-2 Encoder

| input I_0	input I_1	input I_2	input I_3	output O_1	output O_0
1	0	0	0	0	0
0	1	0	0	0	1
0	0	1	0	1	0
0	0	0	1	1	1

one or more chemical inputs. We have been investigating the use of light as inputs and outputs, usually via photochromes that interact photochemically or photophysically with attached chromophores. Photochromes are photochemical switches that may be photoisomerized back and forth between two (meta)-stable states.[20] Recent implementations include a half-adder,[21] 2:1 digital multiplexer,[22] and 1:2 demultiplexer.[23]

A digital encoder converts data into a code. One reason to do this is to compress information for transmission or storage. Consider, for example, the single-bit 4-to-2 encoder, whose truth table is shown in Table 1. The encoder converts 4 bits of data

† Chalmers University of Technology.
‡ Arizona State University.
(1) Ball, P. *Nature (London, U.K.)* **2000**, *406*, 118–120.
(2) Magri, D. C.; Vance, T. P.; de Silva, A. P. *Inorg. Chim. Acta* **2007**, *360*, 751–764.
(3) Tian, H.; Wang, Q. C. *Chem. Soc. Rev.* **2006**, *35*, 361–374.
(4) Venturi, M.; Balzani, V.; Ballardini, R.; Credi, A.; Gandolfi, M. T. *Int. J. Photoenergy* **2004**, *6*, 1–10.
(5) de Silva, A. P.; Uchiyama, S. *Nat. Nanotechnol.* **2007**, *2*, 399–410.
(6) de Silva, A. P.; Uchiyama, S.; Vance, T. P.; Wannalerse, B. *Coord. Chem. Rev.* **2007**, *251*, 1623–1632.
(7) Balzani, V.; Credi, A.; Venturi, M. *ChemPhysChem* **2003**, *3*, 49–59.
(8) Credi, A. *Angew. Chem., Int. Ed.* **2007**, *46*, 5472–5475.
(9) Brown, G. J.; de Silva, A. P.; Pagliari, S. *Chem. Commun. (Cambridge U.K.)* **2002**, 2461–2463.
(10) Pischel, U. *Angew. Chem., Int. Ed.* **2007**, *46*, 4026–4040.
(11) Raymo, F. M.; Giordani, S. *J. Am. Chem. Soc.* **2001**, *123*, 4651–4652.
(12) Niazov, T.; Baron, R.; Katz, E.; Lioubashevski, O.; Willner, I. *Proc. Natl. Acad. Sci. U.S.A.* **2006**, *103*, 17160–17163.
(13) Margulies, D.; Melman, G.; Felder, C. E.; Arad-Yellin, R.; Shanzer, A. *J. Am. Chem. Soc.* **2004**, *126*, 15400–15401.
(14) Liu, Y.; Jiang, W.; Zhang, H. Y.; Li, C. J. *J. Phys. Chem. B* **2006**, *110*, 14231–14235.
(15) Baron, R.; Lioubashevski, O.; Katz, E.; Niazov, T.; Willner, I. *J. Phys. Chem. A* **2006**, *110*, 8451–8456.
(16) Margulies, D.; Felder, C. E.; Melman, G.; Shanzer, A. *J. Am. Chem. Soc.* **2007**, *129*, 347–354.
(17) Frezza, B. M.; Cockroft, S. L.; Ghadiri, M. R. *J. Am. Chem. Soc.* **2007**, *129*, 14875–14879.
(18) Browne, W. R.; De Jong, J. J. D.; Kudernac, T.; Walko, M.; Lucas, L. N.; Uchida, K.; van Esch, J. H.; Feringa, B. L. *Chem.—Eur. J.* **2005**, *11*, 6414–6429.
(19) Strack, G.; Ornatska, M.; Pita, M.; Katz, E. *J. Am. Chem. Soc.* **2008**, *130*, 4234–4235.
(20) Gust, D.; Moore, T. A.; Moore, A. L. *Chem. Commun. (Cambridge U.K.)* **2006**, *2006*, 1169–1178.
(21) Andréasson, J.; Straight, S. D.; Kodis, G.; Park, C.-D.; Hambourger, M.; Gervaldo, M.; Albinsson, B.; Moore, T. A.; Moore, A. L.; Gust, D. *J. Am. Chem. Soc.* **2006**, *12*, 16259–16265.
(22) Andréasson, J.; Straight, S. D.; Bandyopadhyay, S.; Mitchell, R. H.; Moore, T. A.; Moore, A. L.; Gust, D. *Angew. Chem., Int. Ed.* **2007**, *46*, 958–961.
(23) Andréasson, J.; Straight, S. D.; Bandyopadhyay, S.; Mitchell, R. H.; Moore, T. A.; Moore, A. L.; Gust, D. *J. Phys. Chem. C* **2007**, *111*, 14274–14278.
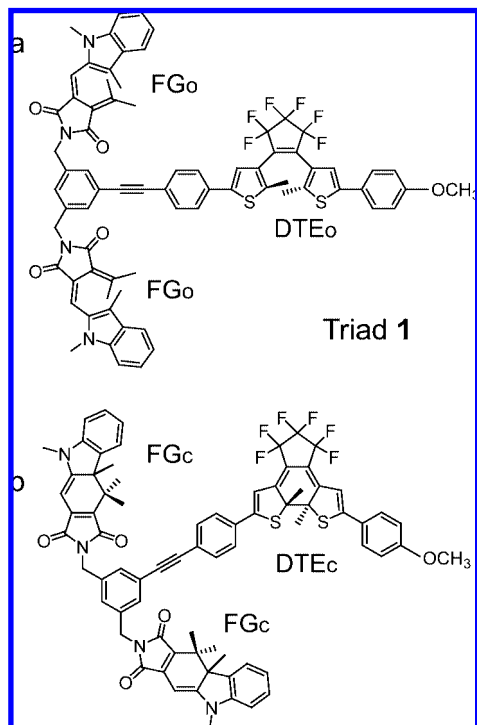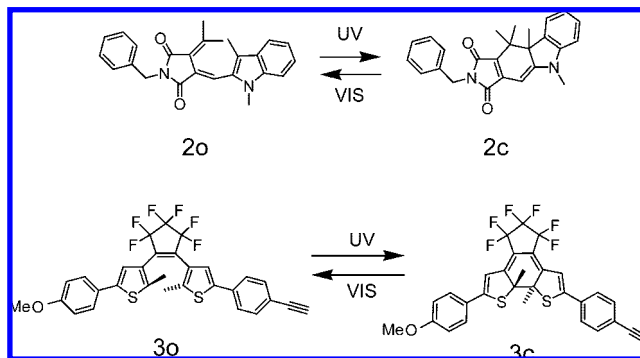
Figure 1. Structures of triad encoder/decoder **1** with all photochromes in the open states that absorb only UV light (a) and in the closed, cyclic states that absorb in the visible (b). The designations FG and DTE indicate fulgimide and dithienylethene moieties, respectively. Although the molecules used in this study were mixtures of racemic compounds, only one enantiomer is shown in the figure.

Figure 2. Structures of fulgimide (**2**) and dithienylethene (**3**) model compounds in the open (left) and closed (right) forms. Although the molecules used in this study were racemic, only one enantiomer is shown in the figure.

Figure 3. Absorption spectra of 2-methyltetrahydrofuran solutions of model compounds **2o** (○), **3o** (■), **2c** (−○−), and **3c** (−■−). The spectra have been scaled to represent the relative populations of chromophores in **1**.

into 2 bits. Each of the four inputs, I_0-I_3, can assume a value of either 0 or 1. The two outputs, O_0 and O_1 comprise a 2-bit binary number (0, 1, 2, or 3 in base-10 mathematics), where O_0 is the sum digit and O_1 is the carry digit. A decoder converts the compressed data back into the original form.
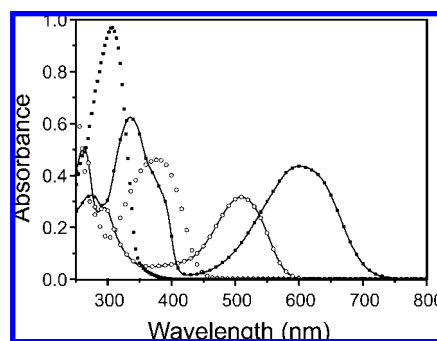
Here, we report molecular triad **1** (Figure 1), which performs as an all-photonic 4-to-2 encoder and 2-to-4 decoder. The molecule consists of a dithienylethene (DTE) photochrome covalently linked to two fulgimide (FG) photochromic moieties. The two kinds of photochromes may be isomerized independently by different wavelengths of light between closed forms which are colored in the visible (Figure 1b) and open, UV-absorbing forms (Figure 1a). The DTE and FG also have absorption maxima at different wavelengths in both the open and closed forms. The closed form of the fulgimide is fluorescent, but when the dithienylethene is also in the closed form, the fulgimide fluorescence is strongly quenched by intramolecular processes. These properties allow the triad to act as either a 4-to-2 encoder or a 2-to-4 decoder, depending upon the nature of the photonic inputs and outputs, as explained in detail below.

Results and Discussion

The synthesis and characterization of triad **1** and its precursors and the details of the spectroscopic measurements are given in the Experimental Section. Here, we will first discuss the photochemistry of two model compounds and then that of the triad. Finally, we will show how these photochemical properties can be employed to achieve the encoder and decoder functions.

Model Compound Spectroscopy. Model FG **2** and DTE **3** (Figure 2) have been previously reported.[24] Fulgimide **2o**, in the open form, exists as a mixture of *E*- and *Z*-isomers that absorb maximally at 380 nm in 2-methyltetrahydrofuran (Figure 3). Irradiation with UV light (e.g., 397 nm) leads to isomerization between the *E*- and *Z*-forms and cyclization of the *E*-form, ultimately converting the sample to a photostationary distribution greatly enriched in the closed form **2c**. This isomer has absorption maxima at 262, 295, and 510 nm). The closed form **2c** fluoresces ($\lambda_{max} = 600$ nm), and single-photon-timing experiments have determined that the excited singlet state has a lifetime of 135 ps.[25] Irradiation of the closed form with visible light induces photoisomerization back to **2o**. Thermal isomerization is not observed on the time scale of these experiments.

The model dithienylethene in the open form, **3o** (Figure 2) has an absorption maximum at 306 nm, with no absorption in the visible (Figure 3). Irradiation in the UV (e.g., 302 nm) isomerizes **3o** to the closed, cyclic form **3c**, which has absorption maxima at 274, 335, and 600 nm (Figure 3). Photoisomerization with visible light converts **3c** back to **3o**, and thermal reversion is not observed.

Triad 1 Spectroscopy. Because the triad contains three photochromes, two of which are identical, it can exist in six photoisomeric forms. The absorption spectra of 2-methyltetrahydrofuran solutions highly enriched in each of the isomers of interest for this investigation are shown in Figure 4.

(24) Straight, S. D.; Liddell, P. A.; Terazono, Y.; Moore, T. A.; Moore, A. L.; Gust, D. *Adv. Funct. Mater.* **2007**, *17*, 777–785.
(25) Straight, S. D.; Terazono, Y.; Kodis, G.; Moore, T. A.; Moore, A. L.; Gust, D. *Aust. J. Chem.* **2006**, *59*, 170–174.
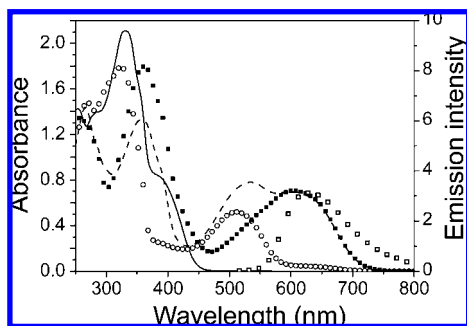
Figure 4. Absorption spectra of a 2-methytetrahydrofuran solution of triad **1** after irradiation with light to produce solutions very highly enriched in FGo−DTEo (—), FGc−DTEo (○), FGo−DTEc (■), and FGc−DTEc (− − −). Also shown is the fluorescence emission at 630 nm from the fulgimide in FGc−DTEo excited at 500 nm (□).

Irradiation of the solution with broad-band green light (460 < λ < 590 nm) yields the triad in which all three photochromes are in the open forms, which do not absorb in the visible. Absorption maxima are observed at 286 (sh), 331, and 387 (sh) nm. This form of **1** will be abbreviated FGo−DTEo, and we will make no distinction between the two equivalent fulgimides. Two fulgimides, rather than one, were incorporated into the molecule in order to enhance some of the effects described below. Irradiation of the solution at 302 nm, where most of the absorption is due to the DTEo chromophore, yields a solution greatly enriched in FGo−DTEc, which has maxima at 362 and 604 nm. Alternatively, irradiating FGo−DTEo at 397 nm photoisomerizes the fulgimides to the closed form, giving FGc−DTEo. Initially, of course, this irradiation produces molecules in which one fulgimide is in the closed form and one is still open, but continued irradiation yields samples in which most of the fulgimides are closed in the photostationary distribution. This material has absorption maxima at 270, 324, and 511 nm (Figure 4). The figure also shows the fulgimide fluorescence emission spectrum of FGc−DTEo, obtained with 500 nm excitation. The emission maximum is at 630 nm. Finally, if FGo−DTEo is irradiated with both 302 and 397 nm light, the sample is converted to a solution highly enriched in FGc−DTEc. The absorption maxima are at 266, 357, 535, and 598 nm.

Figure 4 demonstrates both that it is possible to obtain photostationary distributions very highly enriched in the four photoisomers mentioned above and that the spectra of the triad in its various forms are very similar to linear combinations of the spectra of the model compounds shown in Figure 3. That is, linking the chromophores covalently has not led to strong electronic interactions that influence the absorption spectra.

In the photostationary distribution containing mainly the FGc−DTEc form of the triad, the FGc fluorescence that was apparent in the FGc−DTEo form (Figure 4) and in model compound **2c** is quenched by 98%. This quenching does not lead to sample degradation or the formation of stable photoproducts. It is most likely due to singlet−singlet energy transfer from FGc to DTEc. The overlap of FGc fluorescence and DTEc absorption is excellent, and the interchromophore separations are such that energy transfer by the Förster mechanism is expected to be very rapid. Because DTEc is essentially nonfluorescent, energy transfer could not be confirmed by fluorescence excitation spectroscopy. Calculations using Förster theory (Φ_F of FGc = 0.005, ε_{600} of DTEc = 2×10^4 M^{-1} cm^{-1}, orientation factor $\kappa^2 = 0.67$) yield a value for the critical distance R_0 of 23 Å. Molecular mechanics modeling of **1** yields

Table 2. Time Constants (τ) for Photoisomerization Reactions

compd	λ (nm)	τ (s)	compd	λ (nm)	τ (s)
2o → 2c	397[a]	120	**1**, FGo−DTE → FGc−DTE	397[a]	170
2o → 2c	366[b]	30	**1**, FGo−DTE → FGc−DTE	366[b]	6, 100[c]
2c → 2o	green[d]	21	**1**, FGc−DTEo → FGo−DTEo	green[d]	22
3o → 3c	302[e]	4	**1**, FGc−DTEc → FGo−DTE	green[d]	280
3o → 3c	366[b]	47	**1**, FG−DTEo → FG−DTEc	302[e]	4
3c → 3o	green[d]	350	**1**, FG−DTEo → FG−DTEc	366[b]	25
			1, FG−DTEc → FG−DTEo	green[d]	430

[a] 1.6 mW/cm², see the Experimental Section for details. [b] 1.5 mW/cm², see the Experimental Section for details. [c] The decay was biexponential under these conditions. [d] 9 mW/cm², 460 < λ < 590 nm, see the Experimental Section for details. [e] 1.5 mW/cm², see the Experimental Section for details.

Table 3. Inputs and Outputs for Encoder Function

inputs (I) and outputs (O)	λ (nm)	conditions
I_0 and reset	460 < λ < 590 nm	9 mW/cm², 30 min
I_1	397	1.6 mW/cm², 4 min
I_2	302	1.5 mW/cm², 3 s
I_3	366	1.5 mW/cm², 45 s
O_0	475	absorbance
O_1	625	absorbance

a center-to-center distance between the chromophores of 13 Å. The resulting predicted energy transfer efficiency is 97%, which is comparable to that observed experimentally. The Förster calculation predicts that the 135 ps lifetime of the FGc first excited singlet state would be quenched to <4 ps by energy transfer to DTEc. Time-resolved measurements of this lifetime using the single-photon-timing technique yield a lifetime of <5 ps, although the accuracy of this measurement is not high because the instrument response function with which it is convoluted is 30 ps. Photoinduced electron transfer to yield a short-lived charge-separated state is an alternative mechanism. Because the redox potentials of the two moieties are unknown, this mechanism cannot be ruled out.

Isomerization Kinetics. The observed rates for the various photoisomerization reactions in the triad and model compounds depend on the light flux. (The actual photochemical elementary processes typically occur on the subnanosecond time scale.) The time constants for selected processes under the conditions used in the encoder−decoder study are presented in Table 2, along with the conditions. All studies were carried out in 2-methyltetrahydrofuran at ambient temperatures. In general, the time constants for isomerization of the chromophores in the triad are roughly similar to those for the corresponding monomers. An exception is the time constant for conversion of FGc to FGo using green light. In model compound **2c** and when the DTE moiety of the triad is in the open form, this time constant is ∼22 s. However, when the DTE in the triad is in the closed form, the time constant for FGc to FGo increases to 280 s. The reason is the strong quenching of the FGc first excited singlet state by DTEc, which is also responsible for the strong fluorescence quenching mentioned above.

Encoder Function. As mentioned above, a solution of triad **1** in 2-methyltetrahydrofuran functions as a 4-to-2 digital encoder. The initial state, prior to applying any inputs, is FGo−DTEo, where all of the photochromes are in the open forms. This is achieved by irradiation with green light. The triad is reset to this state prior to each input operation. The various inputs and outputs are summarized in Table 3. Applying input I_0 does not lead to any isomerization, and the sample remains in the FGo−DTEo form.
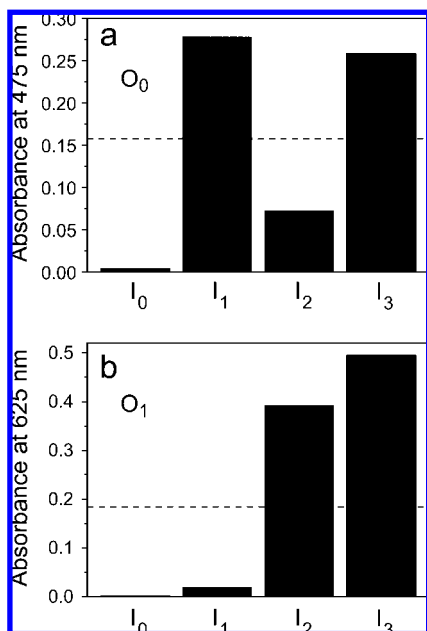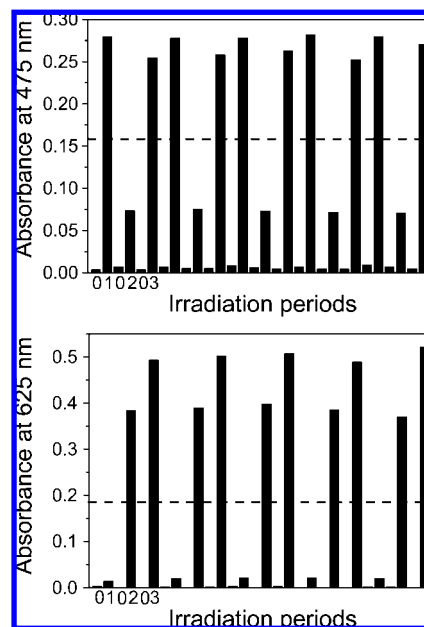
Figure 5. Performance of the triad as a 4-to-2 encoder. The black bars show the absorbance at the appropriate monitoring wavelengths for outputs O_0 and O_1 following application of the four inputs I. The dashed lines are thresholds used to distinguish an *on* output from an *off* output. The variation in height at the top of each bar (barely visible) shows the variation in absorbance during measurement for 5 s.

Figure 6. Photocycling of triad **1** in the encoder mode. The absorbance at 475 nm represents output O_0, and the absorbance at 625 nm represents output O_1. The black bars show the absorbance following repetitive application of inputs I_0, (0), I_1 (1), I_2 (2), and I_3 (3) for five complete cycles. It is apparent that there is no significant degradation of the sample.

Table 4. Truth Table for the 2-to-4 Decoder

input I_1	input I_0	output O_0	output O_1	output O_2	output O_3
0	0	1	0	0	0
0	1	0	1	0	0
1	0	0	0	1	0
1	1	0	0	0	1

Table 5. Inputs and Outputs for Decoder Function

inputs (*I*) and outputs (*O*)	λ (nm)	conditions
reset	$460 < \lambda < 590$ nm	9 mW/cm^2, 30 min
I_0	397	1.6 mW/cm^2, 12 min
I_1	302	1.5 mW/cm^2, 25 s
O_0	535	transmittance
O_1	624	emission, $\lambda_{ex} = 500$ nm
O_2	393	absorbance
O_3	535	absorbance

There is no absorption at the two output wavelengths (475 and 625 nm), and both outputs remain in the 0, or *off* state, corresponding to 0 in base-10 mathematics. Input I_1 isomerizes the triad to mainly the FGc–DTEo form. Therefore, the absorbance at 475 nm is high, whereas that at 625 nm is low. Thus, $O_0 = 1$, and $O_1 = 0$ (1 in base-10). Input I_2 is absorbed by the DTE moiety, and converts the triad solution to mainly FGo–DTEc, giving rise to strong absorption at 625 nm but not at 475 nm. Output O_0 is now 0, and $O_1 = 1$ (2 in base-10). Finally, applying I_3 at 366 nm isomerizes both photochromes to the closed forms (FGc–DTEc), giving high absorbance at both 475 and 625 nm. Both outputs are in the 1 state (*on*), corresponding to the number 3 in base-10.

Thus, the triad solution functions as a 4-to-2 encoder, converting an *on* state for each of the four inputs (I_0–I_3) into the binary representation of a unique base-10 number 0–3 and compressing four bits of data to two, as required by Table 1. The actual performance of the molecule is shown in Figure 5, where Figure 5a shows the absorbance at 475 nm and Figure 5b shows that at 625 nm. The dotted lines in these figures represent convenient thresholds for determining whether the output is *on* or *off*. Unlike an ideal logic gate, any real device must function via a threshold value of some kind. The signal-to-noise obtained is shown by the variation at the tops of the black bars in Figure 5, each of which represents measurement of the absorbance for 5 s. The noise is barely visible and far better than necessary to distinguish *on* from *off*.

Photocycling of the Encoder. To have any hope of being part of a useful device, an encoder must be capable of cycling many times. Although the focus of this research was not the production of technologically useful devices, but rather the realization of scientific principles and possibilities, it was of interest to investigate the photostability of the triad under the conditions used for implementing the encoder. Figure 6 shows the photocycling of the encoder through all four inputs, with resets

between the inputs. This cycle was repeated five times, with no significant degradation of the response at either O_0 (475 nm) or O_1 (625 nm).

Decoder Function. The 2-to-4 decoder converts binary information from two coded inputs, such as those generated by the encoder, to four unique outputs, each of which is either *off* (0) or *on* (1). The truth table is shown in Table 4. Following application of each input combination 00, 01, 10, or 11, (0, 1, 2, or 3 in base-10), the output corresponding to the base-10 number is switched *on*. When triad **1** functions as a decoder, the initial state is FGo–DTEo just as for the encoder. It can be set from any other state of the device with green light. The inputs and outputs for the decoder are listed in Table 5.

The performance of **1** in 2-methyltetrahydrofuran as a decoder is depicted in Figure 7, which shows the response of each output in the initial state and after applying various combinations of inputs. When both inputs are *off*, the sample remains in the FGo–DTEo form. The absorption spectrum (Figure 4) shows
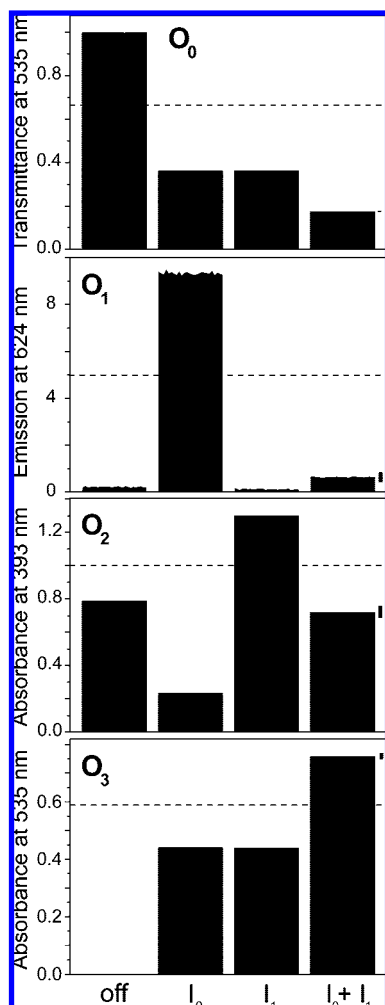
Figure 7. Performance of the triad as a 2-to-4 decoder. The black bars show the signal amplitude at the appropriate monitoring wavelengths for outputs O_0 through O_3 when the inputs are *off*, when I_0 is *on*, when I_1 is *on*, and when both are *on*. The dashed lines are thresholds used to distinguish an *on* output from an *off* output. The variation in height at the top of each bar shows the variation in signal amplitude during measurement for 5 s. The small bars to the right of the tops of the outputs when both I_0 and I_1 are *on* show the variation seen when the order of application of the two inputs is reversed.

virtually no absorbance at wavelengths >470 nm, and with the proper choice of a threshold level (Figure 7) the absorbance at 393 nm is low enough to give an *off* response for O_2. Only low emission intensity is observed at 624 nm upon excitation at 500 nm. Thus, the only output that is *on* is O_0, as the transmittance at 535 nm is close to unity. The system thus represents the first line of the truth table for the decoder.

When I_0 is turned *on*, the sample is isomerized mainly to FGc−DTEo. As can be seen from Figure 4, the presence of the visible absorption band of FGc ($\lambda_{max} \sim 511$ nm) leads to some absorbance at 535 nm. The absorbance is still below the threshold, so that O_3 is still *off*, but strong enough to reduce the transmittance at 535 below the threshold, so that O_0 is now *off*. The absorbance at 393 also decreases, leaving O_2 *off*. However, fluorescence emission from FGc is now observable at 624 nm, and O_1 is *on*. This corresponds to the second line of the decoder truth table.

Alternatively, applying input I_1 at 302 nm isomerizes the triad mainly to FGo−DTEc. The absorbance at 393 nm rises above the threshold because both chromophores absorb there (Figure

4), giving an *on* response for O_2. Both absorbance and transmittance at 535 are below the threshold so that O_3 and O_0 are *off*. There is no significant emission at 624 nm so that O_1 is *off*, and the system represents the third line of the truth table.

Finally, applying both I_0 and I_1 isomerizes both photochromes so that the triad is in mainly the FGc−DTEc form. Because FGc absorbs only weakly at 393 nm, the absorbance there is below the threshold, and O_2 now is *off*. At 535 nm, both FGc and DTEc absorb. This results in switching O_3 *on* and O_0 *off*. Output O_1 is *off* because although FGc is emissive, the excited state is quenched by the closed form of DTE as discussed above, and emission intensity is far below the threshold. Thus, the fourth line of the truth table is represented.

Thus, the decoder function of triad **1** has been demonstrated. The tops of the black bars in Figure 7 show the signal-to-noise level achieved in the measurements, which is far greater than necessary to meet requirements. Absorbance and emission were both monitored for 5 s. When I_0 and I_1 are applied simultaneously, the output amplitudes are a weak function of the order of application of the inputs. The variation due to this factor is shown in Figure 7 and is clearly too small to affect function.

Photocycling of the Decoder. Figure 8 shows the results of experiments to determine the photostability of the triad under decoder operating conditions. Each input−output combination was preceded by a reset operation with green light. There is a slight amount of performance degradation after five cycles. This is due mostly to photodecomposition of DTE.

Conclusions

This research shows that a single molecular species can act both as a 4-to-2 encoder and a 2-to-4 decoder, using only optical inputs and outputs. In addition to performing a relatively complex mathematical operation, the triad can be reconfigured in situ simply by enabling a different set of inputs and outputs. This ability to be reconfigured is often a characteristic of chemical logic gates. The use of only optical inputs and outputs means that no material access to the gate element is necessary, permitting in principle monolithic three-dimensional arrays of devices. Achieving the encoder and decoder functions in a single molecule is logically complex. In the decoder, for example, only one of the outputs is switched on for each input combination. This means that I_0 must counteract the effect of I_1, and vice versa. At the same time, applying *both* I_0 and I_1 must give rise to a unique new output. This means that the molecule must function simultaneously as one NOR gate, two complementary INHIBIT gates, and one AND gate that all share inputs and initial state. The complexity of function and the reconfigurability are both due in part to the fact that unlike electronic devices, where all inputs and outputs are electronic, molecular photonic systems can use light of different wavelengths, allowing for multiple inputs and outputs that can travel through the same spatial regions.

One could imagine a variety of uses for photonic molecular encoders, decoders, etc., in addition to the kinds of applications now satisfied by their electronic analogs. As mentioned earlier, the times necessary for the various photoisomerization reactions depend on the intensity of the light used; the actual photochemical processes occur during the lifetimes of the photochrome excited states (nanoseconds or less). Much faster switching than that reported in Table 2 would be possible with more intense irradiation. That said, it is unlikely that molecular systems such as that described here will replace traditional electronics for current uses in computing and data communication in the near
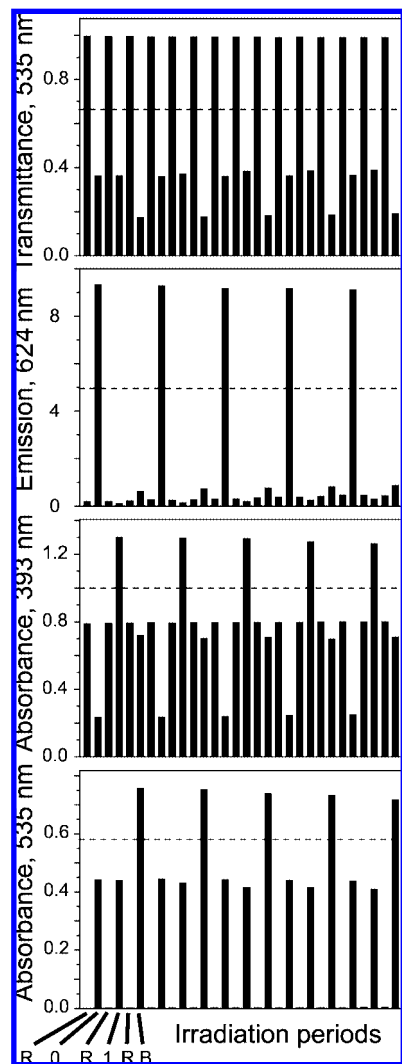
Figure 8. Photocycling of triad **1** in the decoder mode. The signal amplitude for each of the four outputs is shown following five repetitions of the sequence of inputs: reset (R), I_0 (0), reset, I_1 (1), reset, both I_0 and I_1 (B). The sequence is indicated at the bottom of the figure for the first six applications. The dashed lines are thresholds used to distinguish an *on* output from an *off* output. There are small changes over the course of the irradiations that indicate a small amount of decomposition of DTE.

future. However, molecular systems can function in applications where traditional electronics cannot. Examples are the use of optically interrogated molecular logic to label nanoparticles[26] and in a "molecular keypad lock" that could have applications in drug delivery.[16] For the system discussed here, if a sample of nano-objects labeled with suitable decoder molecules were introduced into an organism or other complex system, and each of two spatially distinct sites in the organism were irradiated with one of the two inputs, one could later interrogate the nano-objects with light and determine whether they had visited both, either one, or neither of the irradiated locations simply by reading the outputs. Similar applications on larger scales can also be envisioned.

Experimental Section

Spectroscopic Measurements. Distilled 2-methyltetrahydrofuran was used as the solvent for spectroscopic measurements. The

(26) de Silva, A. P.; James, M. R.; McKinney, B. O. F.; Pears, D. A.; Weir, S. M. *Nat. Mater.* **2006**, *5*, 787–790.
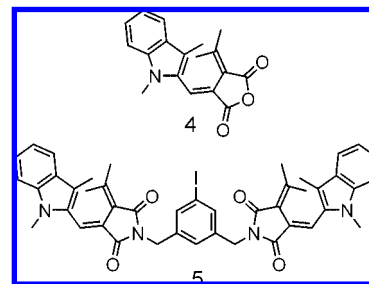
Figure 9. Structures of synthetic intermediate fulgide **4** and fulgimide **5**.

samples were degassed by six freeze−pump−thaw cycles to a final pressure of approximately 10^{-5} Torr. The absorption measurements were performed using a CARY 4000 UV−vis spectrometer. A SPEX Fluorolog $\tau 2$ was used for the emission measurements. After irradiation with the different light input combinations, the inputs were turned off, and the absorbance and the emission were monitored separately using the instruments described above. The sample concentration was ~2.5×10^{-5} M. The 397 nm light and the broad-band green light were generated by a 1000 W Xe/Hg lamp operated at 450 W and equipped with a hot mirror ($A = 1.8$ at 900 nm) to reduce the IR intensity. A 397 nm interference filter was used for the 397 nm light, and a VG 9 glass filter ($A < 1.5$ between 460 and 590 nm) was used for the broad-band green light. The resulting light power densities were ~1.6 mW/cm^2 and ~9 mW/cm^2 for the 397 nm light and the green light, respectively. The 302 and the 366 nm UV inputs were generated by UVP hand-held UV lamps (models UVM-57 and UVGL-25, respectively), each having power densities of 1.5 mW/cm^2. The total sample volume was ~3 mL. With the use of the 397 nm light and the broad-band green light, only one-third of the sample volume was exposed to the light at any one time, whereas the whole sample volume was exposed to 302 and 366 nm light. The samples were stirred continuously during all irradiation processes.

Synthesis. The preparation of 1,3-bis(bromomethyl)-5-iodobenzene and 1-iodo-3,5-bis(*N*-phthalimidomethyl)benzene have been previously described,[27] as has that of fulgide **4** (Figure 9).[28] ^{1}H NMR spectra were recorded on Varian Unity spectrometers at 300 or 500 MHz. Samples were dissolved in deuteriochloroform, with tetramethylsilane as an internal reference, or in toluene-d_8. Mass spectra were obtained on a matrix-assisted laser desorption ionization time-of-flight spectrometer (MALDI-TOF).

Dyad 5. To a suspension of 113 mg (0.22 mmol) of 1-iodo-3,5-bis(*N*-phthalimidomethyl)benzene in 15 mL of ethanol was added 0.7 mL of hydrazine hydrate, and the solution was refluxed under nitrogen for 3 h. The solution was cooled to room temperature, and 30 mL of 2 M HCl was added. After 15 min the solution was poured into 150 mL of 1 M NaOH, and the resulting mixture was extracted four times with dichloromethane. The organic layer was washed with brine and dried over anhydrous K$_2$CO$_3$. The solvent was evaporated, and to the residue was added 140 mg (0.49 mmol) of fulgide **4** and 15 mL of toluene. The solution was stirred under nitrogen at 65 °C overnight. The next day 40 mg (0.29 mmol) of anhydrous ZnCl$_2$ and 400 μL (1.9 mmol) of hexamethyldisilazane were added, and the mixture was again stirred overnight at 65 °C under nitrogen. The reaction mixture was poured into water, and the resulting mixture was extracted twice with toluene and once with dichloromethane. The organic extracts were combined, and the solvent was distilled at reduced pressure. The residue was dissolved in dichloromethane and chromatographed on silica gel, eluting with 25% ethyl acetate in hexanes, to yield 22 mg (0.026

(27) Ryan, T. J.; Lecollinet, G.; Velasco, T.; Davis, A. P. *Proc. Natl. Acad. Sci. U.S.A.* **2002**, *99*, 4863–4866.
(28) Liang, Y.; Dvornikov, A. S.; Rentzepis, P. M. *J. Photochem. Photobiol., A* **1999**, *125*, 79–84.

mmol, 12%) of dyad **5**. ^{1}H NMR (300 MHz, CDCl₃): δ 1.23 (6H, m), 1.94 (3H, s), 1.98 (3H, s), 2.47 (6H, m), 3.89 (3H, s), 3.67 (3H, s), 4.75 (4H, m), 7.11−7.19 (3H, m), 7.25−7.32 (3H, m), 7.48 (2H, s), 7.54−7.62 (3H, m), 7.67 (2H, m). MALDI-TOF: calcd for $C_{44}H_{41}IN_4O_4$ + Na, 839.2; obsd, 839.3. Isotopic distribution: calcd *m/z* (relative intensity) 839.215 (59), 840.218 (33), 841.221 (8); found 839.316 (67), 840.246 (29), 841.209 (4).

Triad 1. A mixture of 2 mL of tetrahydrofuran and 2 mL of triethylamine was bubbled with argon for 1 h, after which time 22 mg (0.026 mmol) of **5** was added along with 30 mg (0.052 mmol) of 1-[5-(4-methoxyphenyl)-2-methylthien-3-yl]-2-[2-methyl-5-(4-ethynylphenyl)thien-3-yl]-3,3,4,4,5,5-hexafluorocyclopentene (**3**),[29] 8 mg (0.026 mmol) of Ph₃As, and 2 (0.002 mmol) mg of Pd₂(dba)₃. The reaction vessel was capped with a septum, and the mixture was stirred overnight at room temperature. The solvent was then evaporated, and the residue was dissolved in dichloromethane and subjected to preparative TLC (2:3 ethyl acetate/hexanes). The appropriate band was scraped off, and the product was extracted from the silica gel with acetone and dichloromethane. The solvent was evaporated, and the residue was again purified by preparative TLC, this time eluting with 1% ethyl acetate in dichloromethane to give 21 mg (0.017 mmol, 64%) of triad **1**. ^{1}H NMR (300 MHz, CDCl3): δ 1.25 (6H, m), 1.96 (12H, m), 2.47 (6H, m), 3.44 (3H, s), 3.68 (3H, s), 3.84 (3H, s), 4.83 (4H, m), 6.92 (2H, d, *J* = 9 Hz), 7.10−7.21 (4H, m), 7.25−7.33 (4H, m), 7.37 (1H, br s), 7.48 (2H, d, *J* = 9 Hz), 7.52 (6H, m), 7.54 (1H, s), 7.56−7.64 (3H, m). MALDI-TOF: calcd for $C_{74}H_{60}F_6N_4O_5S_2$ + Na, 1285.4; obsd, 1285.4. Isotopic distribution: calcd *m/z* (relative intensity) 1285.380 (40), 1286.383 (34), 1287.384 (19), 1288.385 (8); found 1285.377 (45), 1286.342 (35), 1287.308 (15), 1288.331 (6).

(29) Liddell, P. A.; Kodis, G.; Moore, A. L.; Moore, T. A.; Gust, D. *J. Am. Chem. Soc.* **2002**, *124*, 7668−7669.